Coupled, Circumferential Motions of the Cell Wall Synthesis Machinery and MreB Filaments in *B. subtilis*

Ethan C. Garner,[1]* Remi Bernard,[2] Wenqin Wang,[3] Xiaowei Zhuang,[4,3,5]*†
David Z. Rudner,[2]*† Tim Mitchison[1]*†

Rod-shaped bacteria elongate by the action of cell wall synthesis complexes linked to underlying dynamic MreB filaments. To understand how the movements of these filaments relate to cell wall synthesis, we characterized the dynamics of MreB and the cell wall elongation machinery using high-precision particle tracking in *Bacillus subtilis*. We found that MreB and the elongation machinery moved circumferentially around the cell, perpendicular to its length, with nearby synthesis complexes and MreB filaments moving independently in both directions. Inhibition of cell wall synthesis by various methods blocked the movement of MreB. Thus, bacteria elongate by the uncoordinated, circumferential movements of synthetic complexes that insert radial hoops of new peptidoglycan during their transit, possibly driving the motion of the underlying MreB filaments.

The shape of most bacteria is maintained by the cell wall peptidoglycan (PG), a three-dimensional meshwork composed of glycan strands linked by peptide cross-bridges, but how collections of genes confer defined shapes and widths to this structure is unclear. The PG is a single macromolecule, and the mechanisms that localize the synthesis of this structure dictate the shape of the organism.

The peptidoglycan elongation machinery (PGEM) responsible for rod-shaped growth is composed of synthetic enzymes [called penicillin binding proteins (PBPs)] and conserved membrane proteins (MreC, MreD, RodA, RodZ). These proteins interact with MreB (*1*–*4*), a distant actin homolog that assembles into cytoplasmic filaments (*5*, *6*). Depletions of PGEM proteins or disruption of MreB filaments produces round cells (*7*–*9*). MreB appears to form helical structures by light microscopy, which have been proposed to organize the PGEM to facilitate the construction of a rod-shaped cell (*10*–*12*).

MreB is dynamic, and moves directionally in *B. subtilis* (*13*, *14*) and *Caulobacter crescentus* (*15*). However, it is unclear how this motion relates to cell wall synthesis. To explore the origin and function of MreB movement, we characterized and compared the relative dynamics of MreB and the PGEM in *B. subtilis*.

B. subtilis expresses three MreB paralogs (MreB, Mbl, and MreBH). We began by imaging their dynamics with confocal microscopy. Green fluorescent protein (GFP)-Mbl expressed as the sole source of Mbl in the cell displayed well-separated foci that moved linearly across the cell width (Fig. 1A and movies S1, A and B). Maximal intensity projections of these movies revealed closely spaced horizontal bands perpendicular to the cell length, suggesting that the predominant movement occurred as a rotation around the cell circumference. Kymographs drawn across the cell width generated diagonal lines, indicative of circumferential movement occurring at approximately constant velocity (22 ± 4 nm/s, n = 40). Similar circumferential motion was observed with GFP fusion proteins to all three MreB paralogs regardless of expression context (Fig. 1B and movies S2, A and B). The motions of MreB did not arise from rotation of the cell itself: Imaging of MreB and EpsE (a protein associated with the flagellar bodies traversing the cell wall) demonstrated that MreB filaments rotate within a static cell (Fig. 1C and movies S3, A and B).

Previous studies have attributed the motion of MreB to polymerization dynamics or treadmilling (*15*, *16*), models at odds with the observation that purified *B. subtilis* MreB displays no difference in polymerization in adenosine 5′-diphosphate (ADP)- and adenosine 5′-triphosphate (ATP)-bound states (*5*). To investigate the role of polymer dynamics in MreB movement, we imaged GFP-MreB containing two different mutations thought to perturb ATP hydrolysis (*7*, *16*, *17*). Consistent with an inhibition of MreB function, expression of these mutants resulted in perturbed cell morphologies (fig. S1). However, these mutants displayed circumferential movements at speeds similar to those observed above (24 ± 4, 26 ± 3 nm/s; n = 25) (Fig. 1B, fig. S1C, and

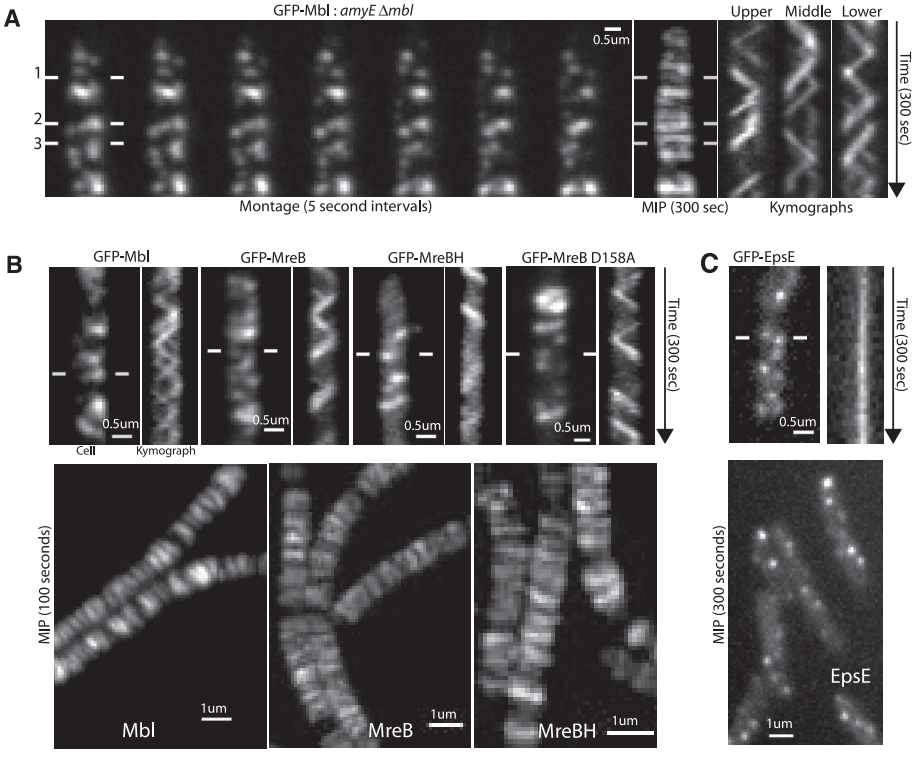

Fig. 1. MreB paralogs display circumferential motion independent of the cell body. (**A**) (Left) Montage of GFP-Mbl motion (BDR2061) from movie S1B. (Middle) Maximal intensity projection (MIP) of movie S1B. (Right) Kymographs drawn between lines in montage. Under our growth conditions, *Bacillus* grows in long septate chains. (**B**) (Top) Kymographs of GFP-Mbl, GFP-MreB, and GFP-MreBH in merodiploid strains. (Far right) Kymograph showing axial motion of GFP-MreB(D158A), a mutation believed to inhibit ATP hydrolysis. (Bottom) MIP of movies of GFP-Mbl, GFP-MreB, and GFP-MreBH. (**C**) (Top) Kymograph of EpsE-GFP. (Bottom) MIP of an EpsE-GFP movie.

[1]Department of Systems Biology, Harvard Medical School, Boston, MA 02115, USA. [2]Department of Microbiology and Molecular Genetics, Harvard Medical School, Boston, MA 02115, USA. [3]Department of Physics, Harvard University, Cambridge, MA 02138, USA. [4]Department of Chemistry and Chemical Biology, Harvard University, Cambridge, MA 02138, USA. [5]Howard Hughes Medical Institute, Harvard University, Cambridge, MA 02138, USA.

*To whom correspondence should be addressed. E-mail: ethan.garner@hms.harvard.edu (E.C.G.); zhuang@chemistry.harvard.edu (X.Z.); rudner@hms.harvard.edu (D.Z.R.); timothy_mitchison@hms.harvard.edu (T.M.)
†These authors contributed equally to this work.

movies S2B and S4), suggesting that a mechanism other than polymerization dynamics drives MreB motion.

Because MreB interacts with the PGEM (*1*–*4*), we hypothesized that MreB movement could be driven by cell wall synthesis. To test this, we monitored GFP-Mbl dynamics while depleting three components of the PGEM: RodA, RodZ, and Pbp2A (Fig. 2A, fig. S2, and movies S5, A to F). As these proteins depleted over time, we observed a gradual cessation of movement. At late stages of depletion, most of the Mbl was motionless. Notably, these experiments revealed a disconnected structure: At intermediate depletion states (~2 hours), cells displayed immobile filaments, while adjacent particles still underwent rotary movement.

Similar to genetic depletions, the addition of antibiotics targeting different steps in PG synthesis caused a cessation of filament motion (Fig. 2B and movies S6, A to D). This effect was rapid: Antibiotic addition to cells under thin agar pads completely stopped filament motion within 10 to 30 s. High concentrations of antibiotics that target other essential processes had no effect on filament movement (Fig. 2C and movies S7, A and B), suggesting that this effect is specific. Furthermore, the minimal inhibitory concentrations (MICs) of antibiotics that stopped motion mirrored the minimal concentrations that inhibited cell growth (fig. S3, table S1, and movies S8, A to D), with short treatments near the MIC resulting in partially frozen filaments.

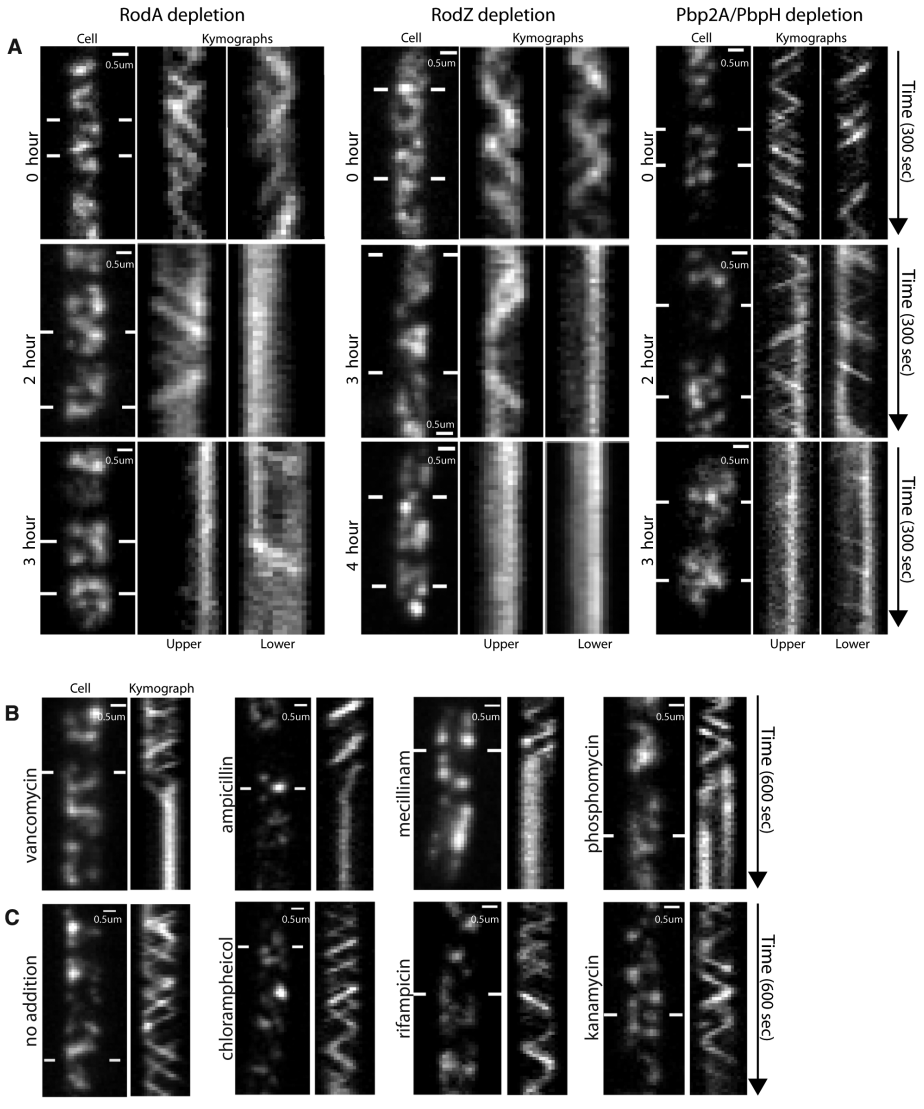

Fig. 2. Filament motion requires cell wall synthesis. (Kymographs are drawn between lines.) (**A**) Kymographs of GFP-Mbl during depletions of isopropyl-β-D-thiogalactopyranoside (IPTG)–inducible genes: (i) RodA, a membrane-spanning component of the PGEM; (ii) RodZ, a protein that links MreB to the PGEM; and (iii) Pbp2A, an elongation-specific transpeptidase, which was depleted in a strain lacking the redundant transpeptidase PbpH. Strains were grown in 2 mM IPTG, shifted to media without IPTG, then imaged at the indicated times. (**B**) Kymographs showing antibiotics targeting cell wall synthesis freeze GFP-Mbl motion. BDR2061 was imaged after addition of 2 μl of antibiotics to a 600-μl agar pad. Initial concentrations: 10 mg/ml ampicillin (blocks transpeptidation), 5 mg/ml mecillinam (blocks transpeptidation), 80 μg/ml vancomycin (blocks transglycosylation and transpeptidation), 50 mg/ml phosphomycin (blocks PG precursor synthesis; 6 μl added). (**C**) Kymographs showing that off-target antibiotics do not affect GFP-Mbl motion. BDR2061 was incubated with the indicated antibiotics for 2 min and immediately imaged. Final concentrations: 500 μg/ml rifampicin (inhibits transcription), 500 μg/ml kanamycin (inhibits translation), 340 μg/ml chloramphenicol (inhibits translation).

Thus, PG synthesis appears to drive the motion of MreB. For this hypothesis to be correct, both the PGEM and MreB paralogs should move around the cell body in a similar manner. To test this, we characterized the dynamics of the MreB paralogs and three of the PGEM components (MreC, MreD, Pbp2A) using high-precision particle tracking. We titrated the expression of GFP fusion proteins to low levels to obtain diffraction-limited foci, which we imaged using total internal reflection fluorescence (TIRF) microscopy to examine their dynamics on the bottom half of the bacterium. Low-level expression was obtained in two ways: (i) with inducible expression in the background of endogenous protein (merodiploids); and (ii) with inducible expression as the only source of protein (replacements). The centroids of foci were fit to obtain positional information with subpixel precision (*18*), and their positions were tracked over time (movie S9A). These studies demonstrated that all six proteins move in linear paths across the cell width (Fig. 3).

We determined the velocity for all traces over 20 frames in length by two methods. These analyses revealed that all six proteins move at similar speeds under each expression condition (Fig. 4, A, B, and G; figs. S6 to S8; and table S2). When the proteins were expressed at low levels as replacements, their mean velocity increased (Fig. 4, A and B), with the exception of the minor paralog MreBH (fig. S9A). This increase in speed may arise from a cellular response to the reduction in the overall levels of the cell wall synthesis machinery, and we could reproduce this effect in trans by tracking merodiploid GFP-Mbl foci in an MreB deletion strain (fig. S9B).

Next, we determined the angles at which these proteins crossed the cell. The mean angle was 90° for all proteins, with most trajectories falling within 15° of this mean (Fig. 4, C and G, and fig. S11). Analysis of the scaling exponents from the mean squared displacement (MSD) versus t plots indicated that all six proteins move in a directed manner (fig. S12 and table S2). Thus, all three MreB paralogs and three PGEM components exhibit directed motions occurring at the same speed and angle to the cell body. Therefore, these proteins move in concert, functioning as a macromolecular unit (*1*–*4*). Consistent with this idea, vancomycin stopped the directed movements of all proteins: Foci of MreB paralogs became immobile, as did chromosomal replacements of MreC and MreD. By contrast, directionally moving

Pbp2A foci transitioned into a rapidly diffusive state (fig. S13 and movie S12A).

Similar to the fragmented structure suggested during PGEM depletions, our single-particle tracking data were not consistent with the existence of a coherent, long-range MreB cytoskeleton. Rather, the directional motions were often discontinuous and independent: Foci of both the MreB paralogs and PGEM displayed pauses and reversals in motion, while adjacent foci continued to move unidirectionally (fig. S14 and movies S12, B to D). These reversals could not have been due to movement of the proteins around the cell body, as our TIRF imaging only reports movements of foci on the bottom half of the cell.

Having observed discontinuous motions of single foci, we next examined the relative directionality between foci to test if their motions were coordinated along the cell length. We calculated the fraction of traces moving in the same direction over the imaging period as a function of their separation. We found no correlation even at the shortest separations: The relative orientations of all proteins were randomly distributed at all distances (Fig. 4D). This uncoordinated movement was evident in our tracking movies (movies S9, A to C, and S10, A to C), and we have high-

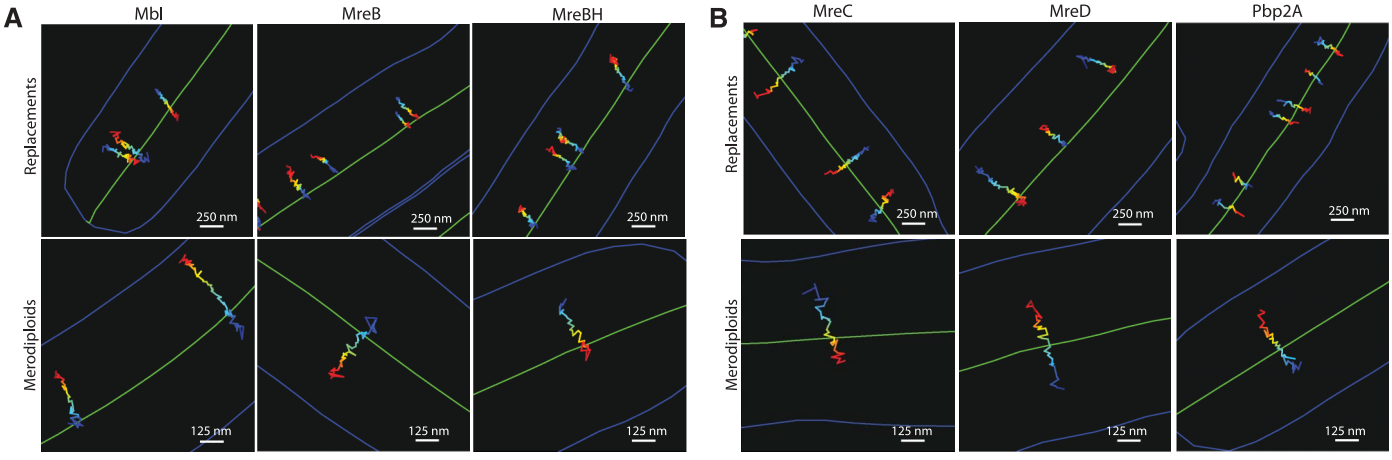

Fig. 3. Particle tracking of MreB paralogs and the PGEM shows linear movements across the cell. Representative traces of (**A**) MreB paralogs and (**B**) PGEM components from each expression condition. Trace color encodes time (blue to red) in 300-ms steps. Cell outline is blue, midline green. Low-level expression of MreB, Mbl, MreC, and MreD in replacements resulted in wider cells, which we stabilized with magnesium (figs. S4 and S5). For the MreB paralogs, both expression methods yielded large numbers of foci that moved in linear paths across the cell width (movies S9, B and C). Expression of PGEM proteins by both methods revealed that PGEM foci partition into two populations, one moving slowly and directionally and one moving rapidly and nondirectionally, which we interpret to be diffusion within the membrane. When expressed at high levels as replacements, a dense mix of both populations was observed. As PGEM expression levels were reduced, the diffusing population effectively disappeared, leaving predominantly directionally moving foci that traversed the cell width (movies S10, A to C). When expressed at low levels in merodiploids, both populations of PGEM foci were observed, with the directionally moving population comprising the minority (movie S11). Because we could only accurately track the slow directionally moving particles, all our data refer to this population.

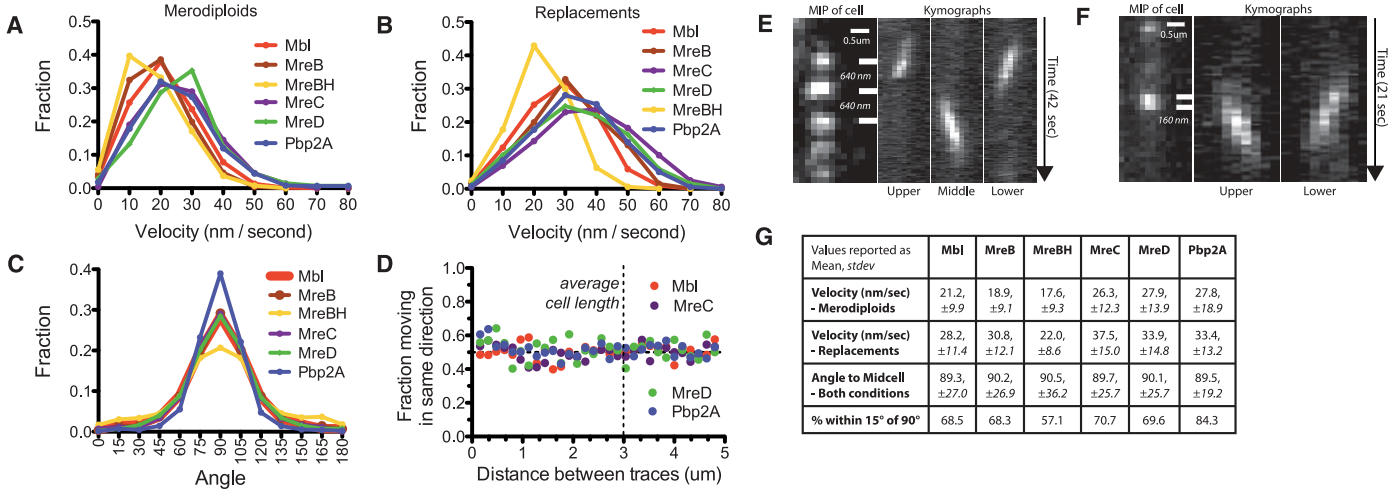

G

Values reported as Mean, *stdev*	Mbl	MreB	MreBH	MreC	MreD	Pbp2A
Velocity (nm/sec) - Merodiploids	21.2, *±9.9*	18.9, *±9.1*	17.6, *±9.3*	26.3, *±12.3*	27.9, *±13.9*	27.8, *±18.9*
Velocity (nm/sec) - Replacements	28.2, *±11.4*	30.8, *±12.1*	22.0, *±8.6*	37.5, *±15.0*	33.9, *±14.8*	33.4, *±13.2*
Angle to Midcell - Both conditions	89.3, *±27.0*	90.2, *±26.9*	90.5, *±36.2*	89.7, *±25.7*	90.1, *±25.7*	89.5, *±19.2*
% within 15° of 90°	68.5	68.3	57.1	70.7	69.6	84.3

Fig. 4. Relative dynamics of the cell wall synthesis machinery and MreB. Histograms of velocity of GFP fusion proteins expressed as (**A**) merodiploids and (**B**) replacements. Velocity (V) was calculated by fitting MSD versus t (fig. S6) to $MSD = (Vt)^2 + 4Dt$, yielding two distinct populations, high (>5×10^{-4} nm/s) and low (≤5×10^{-4} nm/s) (table S2 and fig. S7). Displayed are high-velocity traces that moved in a consistent manner during their lifetime [>0.95 r^2 fit to log(MSD) versus log(t)]. Plots of all data without r^2 screening are in fig. S7. (**C**) Distributions of the angles that traces cross the cell, determined by combining trajectories with segmented brightfield images (fig. S10) (*17*). Shown are traces combined from both expression conditions over 20 frames in length with linear r^2 fits > 0.5. Separate plots of each expression condition and different r^2 screening criteria are in fig. S11. (**D**) Linear traces [as in (C)] extracted from 100 s of imaging were evaluated pairwise to determine their relative directionality. The fraction of traces moving in the same direction is plotted as a function of distance in bins of 160 nm. (**E** and **F**) Kymographs of proximal foci in merodiploid GFP-Mbl (E) and replacement GFP-Pbp2A (F) strains moving in opposing directions across one surface. Distance between kymograph bars is indicated in italics (See also fig. S15 and movies S13, A to D.) (**G**) Summary table of tracking data.

lighted examples of proximal opposing movements (Fig. 4, E and F; fig. S15; and movies S13, A to D). Thus, PGEM and MreB filaments move in both directions around the cell, and we could not resolve any coordination along the cell length.

It thus appears that the coupled motions of the PGEM and MreB reflect the active process of cell wall synthesis: a circumferential motion of disconnected MreB-PGEM complexes moving around the cell in both directions, synthesizing discrete radial bands of PG oriented perpendicular to the cell length (fig. S16). This model is consistent with the arrangement of *B. subtilis* PG observed by atomic force microscopy (*19*).

MreB filaments are required for elongation-specific PG synthesis (*2*, *20*), suggesting that they are integral components of these translocating machines. These filaments may serve as coordinating scaffolds to link the PGEM to the enzymes that synthesize PG precursors (*1*–*4*, *10*) (fig. S17). We cannot completely rule out the contribution of polymer dynamics to these motions, because there are no methods to inhibit MreB polymerization without disrupting existing filaments. However, we did not observe any directed motion in the absence of PG synthesis, even with high-precision measurements (fig. S13), suggesting that PG synthesis is the predominant process driving these motions. If these motions are driven by MreB polymerization or another process, this would require induction of equivalent rigor states during depletions of all PGEM components and the antibiotic inhibition of PG cross-linking, polymerization, and precursor synthesis.

Rather than a contiguous helical structure, these observations reveal the mobile, fragmented nature of MreB. Thus, although MreB is required for rod-shape maintenance, it cannot function as a cell-spanning structure, much less a coherent "cytoskeleton" in *B. subtilis*. It remains to be determined how the short-range activities of these independent biosynthetic complexes impart a long-range order to the cell wall.

References and Notes

1. T. Kruse, J. Bork-Jensen, K. Gerdes, *Mol. Microbiol.* **55**, 78 (2005).
2. Y. Kawai, K. Asai, J. Errington, *Mol. Microbiol.* **73**, 719 (2009).
3. F. O. Bendezú, C. A. Hale, T. G. Bernhardt, P. A. de Boer, *EMBO J.* **28**, 193 (2009).
4. C. L. White, A. Kitich, J. W. Gober, *Mol. Microbiol.* **76**, 616 (2010).
5. J. A. Mayer, K. J. Amann, *Cell Motil. Cytoskeleton* **66**, 109 (2009).
6. F. van den Ent, L. A. Amos, J. Löwe, *Nature* **413**, 39 (2001).
7. T. Kruse, J. Møller-Jensen, A. Løbner-Olesen, K. Gerdes, *EMBO J.* **22**, 5283 (2003).
8. L. J. Jones, R. Carballido-López, J. Errington, *Cell* **104**, 913 (2001).
9. Z. Gitai, N. A. Dye, A. Reisenauer, M. Wachi, L. Shapiro, *Cell* **120**, 329 (2005).
10. R. M. Figge, A. V. Divakaruni, J. W. Gober, *Mol. Microbiol.* **51**, 1321 (2004).
11. R. A. Daniel, J. Errington, *Cell* **113**, 767 (2003).
12. R. Carballido-López, *Microbiol. Mol. Biol. Rev.* **70**, 888 (2006).
13. R. Carballido-López, J. Errington, *Dev. Cell* **4**, 19 (2003).
14. H. J. Soufo, P. L. Graumann, *Curr. Biol.* **13**, 1916 (2003).
15. S. Y. Kim, Z. Gitai, A. Kinkhabwala, L. Shapiro, W. E. Moerner, *Proc. Natl. Acad. Sci. U.S.A.* **103**, 10929 (2006).
16. H. J. Defeu Soufo, P. L. Graumann, *Mol. Microbiol.* **62**, 1340 (2006).
17. See supporting material on *Science* Online.
18. R. E. Thompson, D. R. Larson, W. W. Webb, *Biophys. J.* **82**, 2775 (2002).
19. E. J. Hayhurst, L. Kailas, J. K. Hobbs, S. J. Foster, *Proc. Natl. Acad. Sci. U.S.A.* **105**, 14603 (2008).
20. T. Uehara, J. T. Park, *J. Bacteriol.* **190**, 3914 (2008).

Acknowledgments: We thank P. Graumman, J. Errington, R. Carballido-Lopez, D. Kearns, D. Popham, and D. Scheffers for strains; D. Kahne, S. Walker, T. Bernhardt, and T. Uehara for discussions; Q. Justman for editing; S. Layer for inspiration; T. Emonet for MicrobeTracker; and the HMS Nikon Imaging Center for the use of their facilites. Funding was provided by NIH grants R01-GM073831 (D.Z.R.), R01-GM096450 (X.Z.), and R01-GM39565 (T.M.). X.Z. is a Howard Hughes Medical Investigator. E.C.G. was supported by the Helen Hay Whitney Foundation.

Supporting Online Material

www.sciencemag.org/cgi/content/full/science.1203285/DC1
Materials and Methods
SOM Text
Figs. S1 to S17
Tables S1 to S5
Movies S1 to S13
References

25 January 2011; accepted 20 May 2011
Published online 2 June 2011;
10.1126/science.1203285

Processive Movement of MreB-Associated Cell Wall Biosynthetic Complexes in Bacteria

Julia Domínguez-Escobar,[1] Arnaud Chastanet,[2,3]* Alvaro H. Crevenna,[1]* Vincent Fromion,[4] Roland Wedlich-Söldner,[1]† Rut Carballido-López[2,3]†

The peptidoglycan cell wall and the actin-like MreB cytoskeleton are major determinants of cell shape in rod-shaped bacteria. The prevailing model postulates that helical, membrane-associated MreB filaments organize elongation-specific peptidoglycan-synthesizing complexes along sidewalls. We used total internal reflection fluorescence microscopy to visualize the dynamic relation between MreB isoforms and cell wall synthesis in live *Bacillus subtilis* cells. During exponential growth, MreB proteins did not form helical structures. Instead, together with other morphogenetic factors, they assembled into discrete patches that moved processively along peripheral tracks perpendicular to the cell axis. Patch motility was largely powered by cell wall synthesis, and MreB polymers restricted diffusion of patch components in the membrane and oriented patch motion.

The peptidoglycan (PG) layer, or sacculus, which is composed of glycan strands cross-linked by peptide bridges, forms a load-bearing network that maintains bacterial cell shape. Synthesis and chemical composition of PG are well understood (*1*), but the structure of the sacculus and the mechanisms controlling its growth remain elusive. It is currently assumed that the actin-like MreB proteins form filamentous helical structures along the membrane, which direct cell wall growth by positioning multienzyme complexes that mediate sidewall elongation (*2*). These elongation complexes are thought to contain the essential transmembrane proteins MreC and MreD, RodA and RodZ, PG hydrolases, and penicillin-binding proteins (PBPs), the enzymes that catalyze PG elongation and cross-linking (*3*, *4*). Studies using fluorescently labeled vancomycin (Van-FL) have revealed helical incorporation patterns of PG precursors into the sidewall in *B. subtilis* (*5*) and *Caulobacter crescentus* (*6*), but could not resolve the dynamics of cell wall synthesis. We used total internal reflection fluorescence microscopy (TIRFM), a sensitive method for studying events at cell surfaces (*7*, *8*), to observe the dynamics of the MreB cytoskeleton and its relationship with cell wall growth.

Functional green fluorescent protein (GFP) fusions to the three MreB isoforms in *B. subtilis* (MreB, Mbl, and MreBH) expressed at wild-type levels (fig. S1) formed discrete patches in exponentially growing cells (Fig. 1A). Patches were restricted to the cell periphery (fig. S2A) and exhibited continuous movement along linear tracks roughly perpendicular to the long axis of the cell (Fig. 1B and movie S1). To reconcile our findings with the helical structures described for MreB proteins (*2*, *9*), we simultaneously imaged cells by TIRFM and conventional epifluorescence. Owing to the increased depth of field, MreB patterns visualized by epifluorescence could be misinterpreted as "helical" (Fig. 1C). In addition, MreB localized to transverse bands as cells entered stationary phase (fig. S2B). We found

[1]Max Planck Institute of Biochemistry, Am Klopferspitz 18, D-82152 Martinsried, Germany. [2]INRA, UMR1319 Micalis, F-78352 Jouy-en-Josas, France. [3]AgroParisTech, UMR Micalis, F-78350 Jouy-en-Josas, France. [4]INRA, UR1077 Mathématique, Informatique et Génomes, F-78352 Jouy-en-Josas, France.

*These authors contributed equally to this work.
†To whom correspondence should be addressed. E-mail: wedlich@biochem.mpg.de (R.W.-S.); rut.carballido-lopez@jouy.inra.fr (R.C.-L.)